Low-temperature desorption of N2O from NO on rutile TiO 2(110)-1 × 1

ARTICLE *in* THE JOURNAL OF PHYSICAL CHEMISTRY C · APRIL 2014

Impact Factor: 4.77 · DOI: 10.1021/jp501179y

5 AUTHORS, INCLUDING:

Boseong Kim
Ajou University
7 PUBLICATIONS **46** CITATIONS
SEE PROFILE

Yu Kwon Kim
Ajou University
40 PUBLICATIONS **397** CITATIONS
SEE PROFILE

THE JOURNAL OF PHYSICAL CHEMISTRY C

Article

pubs.acs.org/JPCC

Low-Temperature Desorption of N_2O from NO on Rutile TiO_2(110)-1 × 1

Boseong Kim,[†] Zhenjun Li,[‡] Bruce D. Kay,[‡] Zdenek Dohnálek,[‡] and Yu Kwon Kim*,[†]

[†]Department of Energy Systems Research and Department of Chemistry, Ajou University, Suwon 443-749, South Korea

[‡]Chemical and Materials Sciences Division, Fundamental and Computational Sciences Directorate, Pacific Northwest National Laboratory, P.O. Box 999, Mail Stop K8-88, Richland Washington 99352, United States

ABSTRACT: We find that NO dosed on rutile TiO_2(110)-1 × 1 at substrate temperatures as low as 50 K readily reacts to produce N_2O, which desorbs promptly from the surface leaving an oxygen adatom behind. The desorption rate of N_2O reaches a maximum value after 1−2 s at an NO flux of 1.2×10^{14} NO/cm^2·sec and then decreases rapidly as the initially clean, reduced TiO_2(110) surface with ∼5% oxygen vacancies (V_O's) becomes covered with oxygen adatoms and unreacted NO. The maximum desorption rate is also found to increase as the substrate temperature is raised up to about 100 K. Interestingly, the N_2O desorption during the low-temperature (LT) NO dose is strongly suppressed when molecular oxygen is predosed, whereas it persists on the surface with V_O's passivated by surface hydroxyls. Our results show that the surface charge, not the V_O sites, plays a dominant role in the LT N_2O desorption induced by a facile NO reduction at such low temperatures.

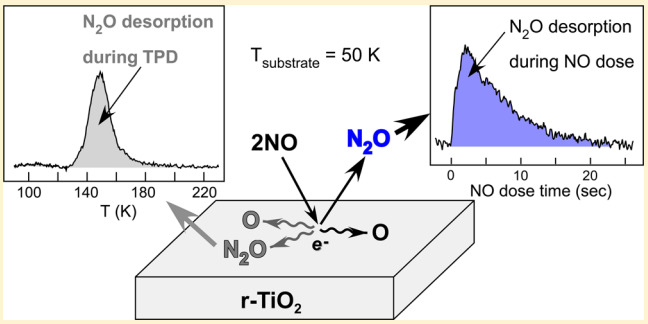

1. INTRODUCTION

NO is a toxic pollutant produced by internal combustion engines that requires reduction to N_2 before the exhaust gas is released to air.[1−3] Considering the growing concern about air pollution by noxious gases, the development of efficient processes and catalysts has been an ongoing challenge.[4−6] Among various oxide-based NO_x catalysts, TiO_2 is not only known to be actively involved in reduction of NO_x, but also is commonly used as a support for various oxides or metal particles.[7−12] In addition, TiO_2 has been reported to be active in photocatalytic NO reduction[13,14] and in NO sensors.[15] Such applications provide a sound motivation for studying the fundamentals of NO interactions with TiO_2. The structural complexity of TiO_2-based industrial catalysts has hampered a detailed atomic level elucidation of the associated catalytic processes and has prompted studies involving model catalysts with atomically well-defined structures such as single crystalline TiO_2 surfaces.[16−18]

It is generally known that NO undergoes reduction into N_2O over TiO_2 under thermal and/or photocatalytic conditions.[13,17,19] Sorescu et al. reported that NO adsorbs weakly on an oxidized TiO_2(110) surface and desorbs at less than 130 K.[17] Above a monolayer coverage (ML) of about 5.5×10^{14} NO/cm^2, partial conversion to N_2O is observed with N_2O desorbing at 170 and 250 K.[17] On the basis of theoretical calculations, a dimeric N_2O_2 species with a stable *cis*-ONNO configuration has been proposed to lead to N_2O formation.[17] The conversion of NO to N_2O has been also reported to occur under UV illumination at 118 K.[13]

On reduced TiO_2(110) with bridging-oxygen vacancy (V_O) defects, reduction of NO to N_2O has been reported to occur readily by releasing one oxygen atom into the V_O.[18,19] This has been confirmed by the suppression of the gap state in the valence band as determined by photoemission measurements and the absence of N-derived species after N_2O desorption.[18] The surface defects can be produced by successive thermal annealing to higher temperatures and N_2O desorption from NO has been observed to increase proportionally with the concentration of defects.[16] Defect sites may transfer electrons from Ti 3d into the π^* orbital of NO efficiently, weakening the N−O bond, thereby facilitating N−O dissociation.[20]

Reduction of NO to N_2O on surface defects has been reported to occur from a very initial NO dose[18,21] and N_2O formation has been observed even at a substrate temperature as low as 110 K.[13] The type and concentration of defects varied widely depending on the preparation methods[16−18] and the uncertainty in the defect structure hampers an unambiguous understanding on the role of surface charge in the NO reduction. Further understanding of how NO dissociates and reduces to N_2O on surface defects may be gained by studying the interaction of NO with a well-ordered TiO_2(110)-1 × 1 surface having well-defined V_O defects. Low substrate temperatures (<100 K) may also provide evidence for possible reaction intermediates in the reduction of NO to N_2O.

In this study, we focus on the role of V_O's in the reduction of NO to N_2O at very low (50 K) substrate temperatures. In these studies, a well-defined molecular beam of NO is impinged onto TiO_2(110) having a finite concentration of V_O's, while the

Received: February 3, 2014
Revised: April 8, 2014
Published: April 11, 2014

   dx.doi.org/10.1021/jp501179y | J. Phys. Chem. C 2014, 118, 9544−9550

substrate temperature is held fixed at a temperature between 50−100 K. Our results show that spontaneous N_2O formation and desorption occurs during the NO dose even at substrate temperatures as low as 50 K. We show evidence that this low temperature (LT) N_2O desorption is mainly induced by the charge at the surface, not just by the V_O sites themselves. To the best of our knowledge, this is the first report of facile N_2O desorption induced by the LT NO reduction on TiO_2 at such low temperatures.

2. EXPERIMENTAL SECTION

The experiments were performed in a UHV molecular beam-surface scattering apparatus which was maintained at a base pressure of 1×10^{-10} Torr.[22] In this study, two different types of sample mounting methods were used. First, a single crystal rutile TiO_2(110) substrate ($10 \times 10 \times 1$ mm^3, Princeton Scientific) was bonded on a 1 mm thick Ta plate of the same size using a high temperature ceramic adhesive (Aremco 503), which was spot-welded to a 1 mm thick Ta wire for a resistive. In this method, the whole TiO_2 crystal surface (1 cm^2) could be under the uniform NO beam flux (1.2×10^{14} NO/cm^2 s), while the lowest temperature achieved was about 70 K.

In the other method, a sample holder with a front Mo retaining ring with inner diameter of about 9 mm was used. The TiO_2 substrate was mounted on the back plate of the sample holder using the ceramic glue and the front Mo retaining ring was fastened onto the TiO_2 surface using a set of screws for a better thermal contact for efficient cooling. In this way, the substrate cooled down to about 50 K. The molecular beam size was reduced to about 7 mm and the sample position during the dose was carefully aligned so that the beam was focused onto the TiO_2 substrate which could be confirmed from a clearly visible watermark obtained from dosing H_2O up to 1000 L at the substrate temperature of 50 K.

Both approaches yielded identical results for the LT N_2O desorption from NO dosed on TiO_2 at temperatures <100 K and corroborated the idea that the observed N_2O desorption is the result of a reaction of NO on TiO_2.

A well-practiced procedure of repeated Ne^+-ion sputtering and annealing to 870 K was used to prepare a rutile TiO_2(110)-1×1 surface with a well-ordered arrangement of bridge-bonded oxygen rows and Ti^{4+} rows. Ordering of the TiO_2(110)-1×1 surface was confirmed from a sharp 1×1 pattern in a low-energy electron diffraction (LEED) measurement. Surface vacancy concentration was quantitatively measured and monitored by H_2O TPD at every stage of the sputter−annealing cycle. The distinct recombinative H_2O desorption peak at 500 K was used as a quantitative measure of the V_O-concentration.[23−25]

Molecular NO (Matheson, CP grade) was dosed using an effusive NO beam maintained at room temperature at substrate temperatures between 50−100 K, while the various mass fragments of possible reaction products such as N_2, N_2O, NO, and NO_2 were also monitored using a quadrupole mass spectrometer (UTI 100C).

3. RESULTS AND DISCUSSION

Figure 1 comparatively shows the TPD spectra of NO (top) and N_2O (bottom) dosed separately on r-TiO_2. Following the NO dose, two reaction products, N_2O and N_2, are observed along with the desorption of unreacted NO. Two peaks are observed in the NO TPD, the first at 100−130 K and the second at ∼270 K. Several distinct peaks can be discerned in

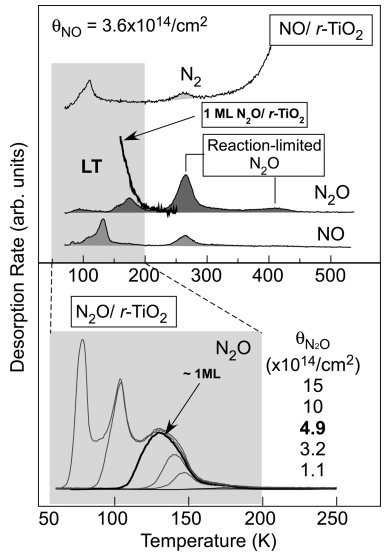

Figure 1. Top: TPD spectra obtained after the NO dose ($\theta_{NO} = 3.6 \times 10^{14}$ NO/cm^2) on r-TiO_2 at 50 K showing the desorption of NO, N_2O and N_2 as observed at 30, 44, and 28 amu. The trailing edge of the N_2O TPD spectrum from near 1 ML (4.9×10^{14} N_2O/cm^2) of N_2O dosed on TiO_2 (bold line) is also drawn (top) for comparison with that from NO/r-TiO_2. Bottom: N_2O TPD spectra (m/z = 44 amu) following different N_2O doses on r-TiO_2 at 50 K.

the N_2O TPD spectra. Two peaks, the first at 170 K (LT N_2O) and a second at 270 K, are observed at temperatures where NO is still present on the surface, while an additional broad peak with a maximum at 400 K is observed after NO is gone. N_2 desorption is superimposed on a background signal of m/z = 28 amu and only the peak at 270 K is identified as being the reaction product of NO reduction.

N_2O dosed on r-TiO_2 does not yield any reaction products in TPD experiments[26] and desorbs at fairly low temperatures (<150 K) with a desorption tail extending to 200 K (see the bottom panel as well as the bold line in the top panel of Figure 1). Since unreacted NO desorbs at 100−140 K, the diffusion of N_2O may be limited by the presence of NO at lower temperatures (<140 K). This may induce desorption of N_2O (∼100 K) even before the high temperature N_2O desorption states (160−180 K) are saturated. Compare the LT N_2O desorption states with that of N_2O dosed on r-TiO_2 in a bold line in the top panel of Figure 1. The detailed shapes of the LT N_2O desorption peaks are strongly influenced by coadsorbed species such as oxygen adatoms, surface hydroxyls, and NO (see below for further discussion). Thus, the LT N_2O desorption states observed below 200 K (the top panel of Figure 1) from NO on r-TiO_2 are likely to originate from N_2O produced from NO bound to TiO_2 at lower temperatures, and desorbing from Ti^{4+} sites (∼100 K) and defects (V_O's on r-TiO_2 and/or oxygen adatoms on o-TiO_2) (160−180 K).[26]

The N_2O desorption peaks above 200 K arise from reaction-limited processes involving NO-derived adsorbates since molecular N_2O desorption occurs well below 200 K. Multiple desorption peaks over a wide range of temperatures (up to 400 K) suggest that multiple reaction channels are involved in the reactions of NO on r-TiO_2.

Figure 2(a) shows a time dependent desorption signal of N_2O (m/z = 44) measured during the NO dose at various substrate temperatures (50−100 K). The N_2O signal increases promptly as the NO beam impinges (time = 0 s) onto r-TiO_2

dx.doi.org/10.1021/jp501179y | J. Phys. Chem. C 2014, 118, 9544−9550

and reaches a maximum rate after about 1−2 s. After the maximum desorption rate is achieved, the signal decreases rapidly and vanishes at longer NO doses. The maximum N_2O desorption rate increases as the dose temperature is increased (Figure 2(a)).

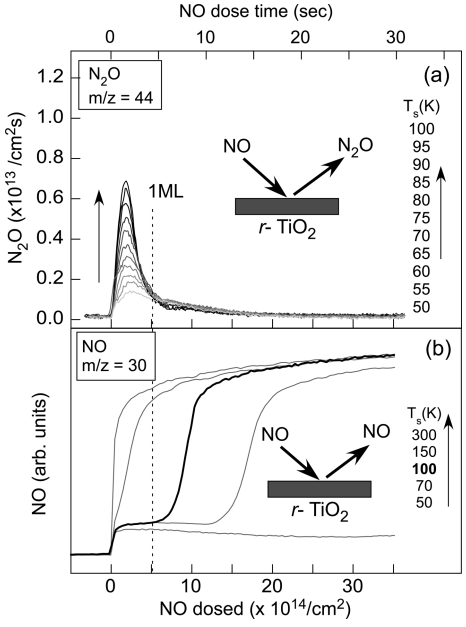

Figure 2. N_2O (m/z = 44 amu) (a) and NO (m/z = 30 amu) (b) desorption rates as a function of NO dose (NO dose time is also indicated) on r-TiO_2 (V_O's concentration ≈ 5%) at different temperatures. The NO flux is set to 1.2×10^{14} NO/cm^2 s. The maximum N_2O desorption rate increases with increasing substrate temperature. Also shown is the NO uptake curve (b) during the NO dose at T_s = 50−300 K. It shows that NO sticks on the r-TiO_2 when the N_2O desorption occurs (a) up to T_s = 100 K.

We also note that the NO uptake curves (Figure 2(b)) taken simultaneously over the same temperature range (50−100 K) show that NO saturation does not occur during the time period (~5 s) when facile N_2O desorption is observed. Thus, the observed N_2O desorption clearly results from submonolayer coverages of adsorbed NO. This point is further discussed below.

The unambiguous assignment of the m/z = 44 amu signal to N_2O (vs CO_2) desorption is confirmed by the identical temporal dependence of the m/z = 14 amu but not the m/z = 12 amu TPD signals (not shown). The absolute desorption rate of N_2O in number of molecules/cm^2 s is calculated by measuring the signal intensity of N_2O scattered from the TiO_2 substrate under a known flux of N_2O (1.2×10^{14} N_2O/cm^2 s) at 300 K.

N_2O desorption during the NO dose is nearly completed by the saturation dose (~5 s) at the dose temperatures of 50−100 K and the N_2O desorption rate vanishes at longer NO doses. As the desorption of N_2O during the NO dose is most likely the result of reductive coupling between two adsorbed NO molecules, oxygen adatoms (O_a's) have to be left on the TiO_2 surface since no O_2 desorption is detected during the NO dose. (The role that the O_a's may play in the surface-catalyzed reduction of NO to N_2O is further explored below.) The $N_2O(g)$ formation from $2NO(a)$, that is, $2NO(a) \rightarrow N_2O(g) + O_a$, is estimated to be highly exothermic (at least −120 kJ/mol).[27] We believe that the heat released during the reaction can facilitate the desorption of N_2O molecules as their desorption energy from Ti^{4+} sites is only 27−32 kJ/mol.[17,28]

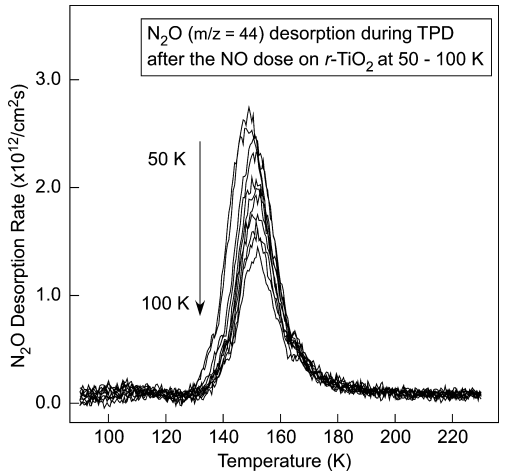

Figure 3. TPD spectra showing desorption of N_2O after the NO dose on r-TiO_2 at T_s = 50−100 K (see Figure 2) The N_2O desorption at low temperature regime (LT N_2O) decreases as the dose temperature is increased to 100 K.

Figure 3 shows TPD spectra of N_2O after the NO dose at 50−100 K that is shown in Figure 2. We find a distinct N_2O desorption peak centered at 170 K. Because the LT N_2O peak (<200 K) is desorption-limited, the LT N_2O desorption during the TPD is likely to be due to N_2O formation during the NO dose at lower temperatures (50−100 K). Thus, this result suggests that some of the N_2O molecules produced during the dose do not desorb and are bound to the surface until they desorb at higher temperatures (up to 200 K) during TPD.

We further note that the area of the LT N_2O desorption peak at 170 K decreases as the substrate temperature is raised from 50 to 100 K. This is in contrast with the increasing N_2O desorption during the NO dose with increasing dose temperatures (Figure 2). These complementary data further support the idea that both the LT N_2O desorbed during the dose (Figure 2) and postdose TPD (Figure 3) originate from the same catalytic LT reduction process of NO on TiO_2 at 50−100 K.

The integrated amounts of N_2O both during the NO dose (N_2O_a, from Figure 2) and during the subsequent TPD (N_2O_b integral from 100−200 K, from Figure 3) are plotted in Figure 4. The N_2O_a integral increases from 1 to 2×10^{13} N_2O/cm^2 as the dose temperature increases from 50 to 100 K. As already

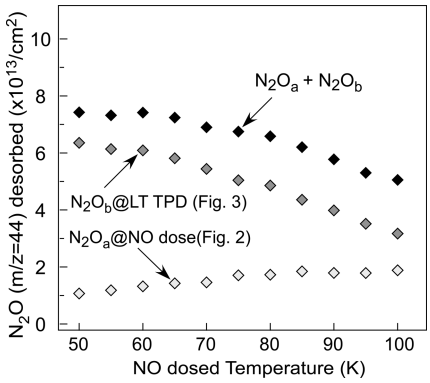

Figure 4. The integrated amounts of N_2O desorbed during the NO dose on r-TiO_2 (N_2O_a, from Figure 2) as well as during the subsequent TPD (N_2O_b, integral from 100−200 K, from Figure 3) plotted as a function of dose temperature.

dx.doi.org/10.1021/jp501179y | J. Phys. Chem. C 2014, 118, 9544−9550

discussed, the enhanced N_2O desorption is likely due to exothermicity-driven desorption of N_2O. In contrast, N_2O_b decreases from 6.4×10^{13} to 3.2×10^{13} N_2O/cm^2. The decrease of N_2O_b is higher than the increase of N_2O_a, which results in a net decrease ($\sim 2 \times 10^{13}$ N_2O/cm^2) of the sum ($N_2O_a + N_2O_b$). This result is in conflict with our expectation and the origin of this decrease is uncertain. It may be that the overall LT N_2O formation yield is reduced as the temperature is raised to 100 K or possibly be a result of differences in the angular distribution of N_2O desorbing during the NO dose and during the subsequent TPD at 50−100 K. As our QMS is positioned in a line-of-site, we do not measure an angularly integrated desorption signal.

The surface coverage of NO also changes as the dose temperature is raised from 50 to 100 K. During the extended dose (up to 60 s) of NO (Figure 2), multilayers of NO may grow at 50 K, but the surface coverage of NO becomes limited to a monolayer at 100 K (Figure 2). The decreasing equilibrium surface coverages of NO as the substrate temperature is raised from 50 to 100 K may limit the overall yield ($N_2O_a + N_2O_b$) of N_2O formation from NO at the low temperatures.

Figure 5 compares the LT N_2O desorption at 90 K from the r-TiO_2 substrate with those from other chemically modified

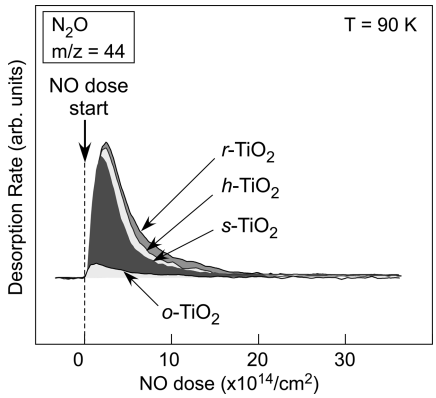

Figure 5. Comparison of N_2O ($m/z = 44$) desorption rates during the NO dose on modified TiO_2 surfaces such as r-TiO_2, h-TiO_2, s-TiO_2, and o-TiO_2 at 90 K. The N_2O desorption rate on o-TiO_2 is notably suppressed under the same dose condition.

TiO_2 surfaces. Here, V_O's on the TiO_2(110) surface are treated with H_2O (and O_2) prior to the NO dose to obtain substrates with V_O's passivated by surface hydroxyls (h-TiO_2) or oxygen atoms (s-TiO_2). h-TiO_2 is prepared by dosing 2 ML of H_2O on r-TiO_2 at 70 K followed by annealing to 400 K.[23,29] s-TiO_2 is obtained by exposing the h-TiO_2 to 10^{15}−10^{16} O_2/cm^2 at 300 K. Oxidation of r-TiO_2 with molecular O_2 may be performed either by dosing to $\sim 2 \times 10^{15}$ O_2/cm^2 at 300 K or a dose of $1-5 \times 10^{14}$ O_2/cm^2 at 50 K followed by annealing to 300 K.[29,30] The resulting surface (o-TiO_2) has a negligible amount of V_O's (passivated by oxygen atoms) with some oxygen adatoms on Ti^{4+} sites.

We find that the initial N_2O desorption rates are very similar among r-TiO_2, h-TiO_2, and s-TiO_2, although the total amount of N_2O desorbed is slightly decreased in the order of r-TiO_2 > h-TiO_2 > s-TiO_2. This result suggests that the passivation of the V_O sites does not significantly quench the LT NO reduction channel away and that TiO_2 surfaces with the V_O sites passivated by OH (h-TiO_2) or O (s-TiO_2)[23−25] can still induce the LT N_2O desorption, although the passivation has a slight influence on the total amount of N_2O. Thus, it leads us to the fact that *the charge associated with V_O sites on r-TiO_2 as well as on h-TiO_2 and s-TiO_2 induces the facile LT NO reduction to N_2O and the instantaneous desorption of N_2O at such low temperatures.*

The dramatic decrease of the N_2O desorption on o-TiO_2 (Figure 5) indicates that the presence of oxygen adatoms on o-TiO_2 can readily suppress the facile LT N_2O formation (and desorption) channel. This is consistent with the observation that the N_2O desorption from r-TiO_2 is quenched away after ∼5 s of NO exposure (Figure 2) due to the accumulation of oxygen adatoms on the surface after the LT N_2O formation.

The results from o-TiO_2 in Figure 5 further corroborate the idea that the surface charge on the TiO_2 surface is crucial in the LT N_2O formation. The coverage of the oxygen adatoms on the o-TiO_2 is far less (∼5%) than the total number of Ti^{4+} sites ($5.2 \times 10^{14}/cm^2$) and therefore there is an abundance of Ti^{4+} sites available for the incoming NO for a subsequent reaction; H_2O TPD from o-TiO_2 shows a ML-H_2O desorption peak with an intensity comparable to that of r-TiO_2. Instead, dissociative adsorption of molecular O_2 over V_O's depletes both the V_O's and the surface charges.[29,31] As a result, nearly no surface charge is left on o-TiO_2, while h-, s-, and r-TiO_2 surfaces have surface charge located on Ti^{4+} sites.[29,31−34] This result suggests that the surface charge associated with V_O's is driving the LT NO reduction to N_2O and its subsequent desorption.

The TPD spectra taken after the NO dose in Figure 5 are compared in Figure 6(a). The N_2O desorption peak around

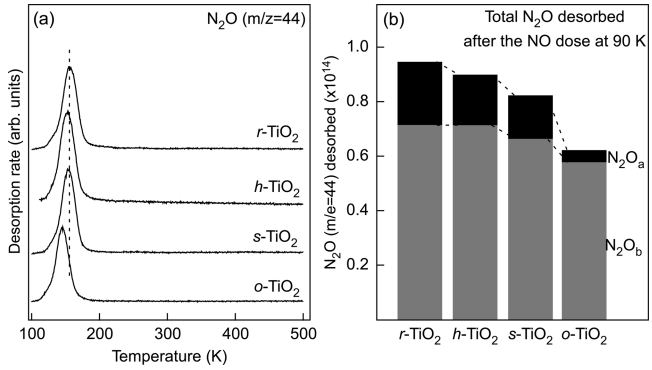

Figure 6. (a) TPD spectra showing desorption of N_2O after the NO dose (Figure 5) on various TiO_2 surfaces of r-TiO_2, h-TiO_2, s-TiO_2, and o-TiO_2 at T_s = 90 K. (b) The integrated amounts of N_2O desorbed during the NO dose (N_2O_a, from Figure 5) as well as during the subsequent TPD (N_2O_b, integral from 90−200 K, from the left panel) are compared.

160 K arises from desorption of the remaining LT N_2O produced by the LT NO reduction. The intensity of the peak is quite similar among r-TiO_2, h-TiO_2, and s-TiO_2. In contrast, the peak maximum shifts slightly to ∼150 K with a decrease in intensity on o-TiO_2. Such a variation in the LT N_2O desorption profile is observed to be strongly dependent on the type of surfaces (r-, h-, s-, and o-TiO_2) and on the dose temperature; compare the LT N_2O TPD profiles in Figures 1,3, and 6. This observation is interpreted to be due to the fact that the LT N_2O is formed at lower temperatures and desorbs during TPD as the substrate temperature is raised (desorption-limited process); that is, the desorption of N_2O is strongly influenced by the local environment around the adsorption sites.

The integrated amount of the LT N_2O (N_2O_b) in the TPD spectra of Figure 6(a) combined with the N_2O desorbed during

dx.doi.org/10.1021/jp501179y | J. Phys. Chem. C 2014, 118, 9544−9550

the NO dose (Figure 5, N_2O_a) is compared in Figure 6(b). This figure shows that N_2O_b as well as N_2O_a decreases clearly on *o*-TiO_2. It is interpreted as a result of the decrease in the surface charges due to the buildup of oxygen adatoms on *o*-TiO_2. Both N_2O_a and N_2O_b are quite similar between *r*-TiO_2 and *h*-TiO_2. This observation clearly shows that the occupation of the oxygen vacancy with a surface hydroxyl has little effect on the overall LT N_2O yield. On *s*-TiO_2, the overall LT N_2O yield is less than that on *r*-TiO_2 (or *h*-TiO_2), probably due to an accumulation of trace of oxygen adatoms during the O_2 scattering at RT.

The total N_2O yield from *r*-TiO_2 in Figure 6 is about $9 \times 10^{13}/cm^2$, whereas that in Figure 4 is only about $7 \times 10^{13}/cm^2$. The two results are obtained from two different TiO_2(110) crystals as described in the Experimental Section. However, the surface oxygen vacancies are measured to be about $2.6 \times 10^{13}/cm^2$ on both surfaces. This indicates that there is a sample-to-sample variation in the absolute LT N_2O yield of about 20−30%, which may be due to a contribution of uncontrolled defects such as steps and oxygen adatoms.

The dramatic decrease of N_2O_a on *o*-TiO_2 correlates with the fact that the surface charge is nearly depleted on this substrate. However, it is rather surprising that the decrease of N_2O_b on *o*-TiO_2 compared to that on *r*-TiO_2 is only about 20% (Figure 6(b)). Two factors may be considered: First, only a fraction of N_2O that formed during the isothermal scattering escapes the surface as a result of the competition between converting the reaction energy into the translational energy of desorbing N_2O and/or dissipating it into the TiO_2 lattice. Second, further reactions of NO into N_2O may be induced during TPD as more thermal energy becomes available and the mobility of the subsurface charge increases. This has been also observed on fully oxidized TiO_2 by Yates et al.[17]

The role of Ti^{4+} sites on the LT NO reduction can be further tested by predosing H_2O on the *h*-TiO_2 surface. Figure 7 shows

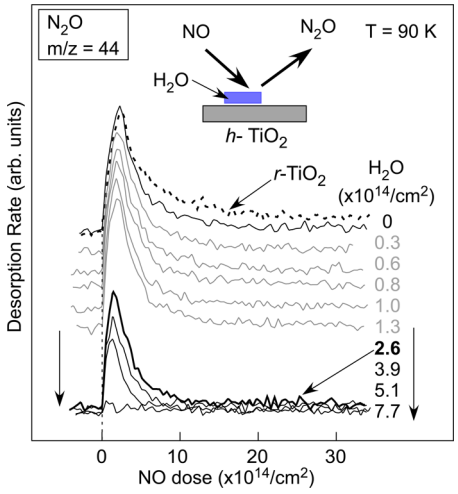

Figure 7. Comparison of the N_2O (m/z = 44) desorption rates measured during the NO dose on H_2O-predosed *h*-TiO_2 at 90 K with increasing $\theta(H_2O)$. The N_2O desorption profile from *r*-TiO_2 (dotted line) and *h*-TiO_2 (thin solid line, $\theta(H_2O)$ = 0) are shown for comparison. The N_2O desorption rate is reduced notably above an H_2O coverage of about 2.6×10^{14} molecules/cm^2.

the N_2O desorption rates measured during the NO dose on *h*-TiO_2, but this time, with increasing amounts of predosed H_2O (from 0 to nearly 2 ML). We find again that the initial desorption rate is not much influenced by the presence of hydroxyls on V_O's. In addition, increasing the H_2O dose up to about $2.6 \times 10^{14}/cm^2$ (~0.5 ML) does not suppress the initial N_2O desorption significantly. A H_2O coverage higher than 0.5 ML does have an effect of suppressing the N_2O desorption and nearly no N_2O desorption is achieved for water coverages above 1 ML.

The observation of suppression of the N_2O desorption from H_2O-covered TiO_2 is a direct result of blocking Ti^{4+} sites with H_2O. The Ti^{4+}-bound H_2O is not likely to be displaced by the impinging NO and effectively suppresses the interaction between impinging NO and the Ti^{4+} sites since H_2O is strongly bound to the Ti sites; it desorbs at ~260 K. Nearly 1 ML of H_2O is found to completely suppress the LT N_2O desorption. From Figure 7, we may also argue that surface charge can induce the LT NO reduction into N_2O (and desorption) only when the impinging NO is in direct contact with the surface Ti sites at the dose temperature.

Figure 8 shows the changes in the N_2O desorption rate when O_2 is predosed on *r*-TiO_2 at 50 K prior to NO beam exposure

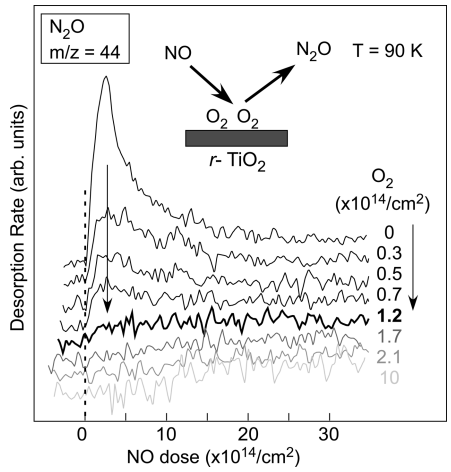

Figure 8. Comparison of N_2O (m/z = 44) desorption rates measured during the NO dose on O_2-predosed *r*-TiO_2 at 90 K. O_2 is dosed at 50 K prior to the NO dose at 90 K. The N_2O desorption rate rapidly decreases from even very low O_2 doses.

at 90 K. As is consistent with the result on *o*-TiO_2 (Figure 5), the N_2O desorption rate is readily suppressed even from the very low O_2 dose of 0.3×10^{14} O_2/cm^2, and it vanishes above an O_2 dose of 1.2×10^{14} O_2/cm^2. This result is strikingly different from that for the case of H_2O in Figure 7, where nearly a ML dose of H_2O is necessary to fully suppress N_2O desorption. The small amount of O_2 (0.3×10^{14} O_2/cm^2) is sufficient to deplete the surface charge, but is far less than that required to cover all of the Ti^{4+} sites. Thus, it further supports the idea that the surface charge is vital for the LT NO reduction and the subsequent N_2O desorption.

Figure 9 shows the variation of the total amount of N_2O_a desorbed during the NO dose (n_{N_2O}) with increasing coverage of predosed H_2O (or O_2). n_{N_2O} decreases very rapidly with increasing dose of O_2, whereas it decreases gradually with increasing H_2O. The rapid reduction in the LT N_2O_a desorption with coadsorbed O_2 is attributed to the depletion of surface charge on the *o*-TiO_2 surface.

The observed role of the surface charge in the LT NO reduction may be understood from a consideration that charge transfer to NO(a) leaves one more electron in the antibonding

dx.doi.org/10.1021/jp501179y | J. Phys. Chem. C 2014, 118, 9544−9550

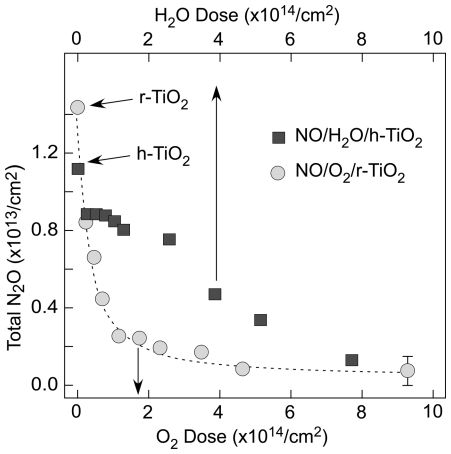

Figure 9. The integrated amount of N_2O_a (n_{N_2O}) desorbed during the NO dose plotted against the amount of predosed O_2 (or H_2O) on *r*-TiO_2 (*h*-TiO_2), respectively. The rapid suppression of the N_2O desorption from O_2-dosed *r*-TiO_2 is compared from that from H_2O-predosed *h*-TiO_2.

orbital (π^*) of NO, resulting in a reduced bond order, thereby facilitating the dissociation of NO.

A possible reaction pathway is proposed to involve a negatively charged intermediate in the form of a dimer, e.g., $(NO)_2^-$. A dimer in the form of $(NO)_2$ has been proposed to be favored between two adjacent NO molecules even in the absence of the surface charge.[17] Charge transfer into $(NO)_2$ would produce $(NO)_2^-$ which would subsequently decompose into O^- (a) and $N_2O(g)$, as shown below.

$$2NO(a) + e^- \rightarrow (NO)_2^-(a) \rightarrow N_2O(g) + O^-(a)$$

Another possibility is that the reaction proceeds by NO dissociation into $N(a)$ and $O(a)$, prior to a subsequent reaction. $O(a)$ is likely to draw more charge since O is more electronegative than N. Thus, $N(a)$ becomes more reactive toward NO to undergo a subsequent reaction into N_2O which may be followed by a desorption. However, dissociation of NO into $N(a)$ and $O(a)$ in this case would be the rate-limiting step toward the LT desorption of N_2O.

The total LT N_2O yield ($7-9 \times 10^{13}$ N_2O/cm^2, Figure 4 and Figure 6) is somewhat higher than the total surface charge ($\sim 5.2 \times 10^{13}$ e^-/cm^2) expected based on the number of surface oxygen vacancies (2.6×10^{13} V_O's/cm^2). We attribute it to the presence of a small amount of additional surface charge that is not related to the surface oxygen vacancies.

4. CONCLUSIONS

We report the unprecedented observation of LT N_2O desorption as a result of spontaneous NO reduction into N_2O at the substrate temperature as low as 50 K. Our quantitative analysis clearly shows that the LT NO reduction to N_2O is mediated by the surface charges associated with the oxygen vacancies (V_O's) on TiO_2. This finding stresses the importance of the surface charge in catalyzing reactions of NO on TiO_2.

AUTHOR INFORMATION

Corresponding Author

*Phone: 82-31-219-2896; fax: 82-31-219-2969; e-mail: yukwonkim@ajou.ac.kr (Y.K.K.).

Notes

The authors declare no competing financial interest.

ACKNOWLEDGMENTS

Part of this work was supported by the U.S. Department of Energy Office of Basic Energy Sciences, Division of Chemical Sciences, Biosciences and Geosciences, and performed at EMSL, a national scientific user facility sponsored by the Department of Energy's Office of Biological and Environmental Research located at Pacific Northwest National Laboratory (PNNL). PNNL is operated for the U.S. DOE by Battelle Memorial Institute under Contract No. DE-AC06-76RLO 1830. Y.K.K. acknowledges financial support from the Basic Science Research Program through the National Research Foundation of Korea (NRF) funded by the Ministry of Education, Science and Technology (NRF-2012R1A1A2007641).

REFERENCES

(1) Odriozola, J. A.; Heinemann, H.; Somorjai, G. A.; de la Banda, J. F. G.; Pereira, P. AES and TDS Study of the Adsorption of NH_3 and NO on V_2O_5 and TiO_2 Surfaces: Mechanistic Implications. *J. Catal.* **1989**, *119*, 71−82.

(2) Forzatti, P. Present Status and Perspectives in de-NO_x SCR Catalysis. *Appl. Catal., A* **2001**, *222*, 221−236.

(3) Qi, G.; Yang, R. T. Performance and Kinetics study for Low-Temperature SCR of NO with NH_3 over MnO_x−CeO_2 Catalyst. *J. Catal.* **2003**, *217*, 434−441.

(4) Pârvulescu, V. I.; Grange, P.; Delmon, B. Catalytic Removal of NO. *Catal. Today* **1998**, *46*, 233−316.

(5) Granger, P.; Parvulescu, V. I. Catalytic NO_x Abatement Systems for Mobile Sources: From Three-Way to Lean Burn after-Treatment Technologies. *Chem. Rev.* **2011**, *111*, 3155−3207.

(6) Busca, G.; Lietti, L.; Ramis, G.; Berti, F. Chemical and Mechanistic Aspects of the Selective Catalytic Reduction of NO_x by Ammonia over Oxide Catalysts: A review. *Appl. Catal., B* **1998**, *18*, 1−36.

(7) Chen, L.; Li, J.; Ge, M. Promotional Effect of Ce-doped V_2O_5-WO_3/TiO_2 with Low Vanadium Loadings for Selective Catalytic Reduction of NO_x by NH_3. *J. Phys. Chem. C* **2009**, *113*, 21177−21184.

(8) Went, G. T.; Leu, L.-J.; Rosin, R. R.; Bell, A. T. The Effects of Structure on the Catalytic Activity and Selectivity of V_2O_5/TiO_2 for the Reduction of NO by NH_3. *J. Catal.* **1992**, *134*, 492−505.

(9) Liu, F.; He, H. Structure−Activity Relationship of Iron Titanate Catalysts in the Selective Catalytic Reduction of NO_x with NH_3. *J. Phys. Chem. C* **2010**, *114*, 16929−16936.

(10) Gao, X.; Jiang, Y.; Fu, Y.; Zhong, Y.; Luo, Z.; Cen, K. Preparation and Characterization of CeO_2/TiO_2 Catalysts for Selective Catalytic Reduction of NO with NH_3. *Catal. Commun.* **2010**, *11*, 465−469.

(11) Tang, F.; Xu, B.; Shi, H.; Qiu, J.; Fan, Y. The Poisoning Effect of Na^+ and Ca^{2+} ions doped on the V_2O_5/TiO_2 Catalysts for Selective Catalytic Reduction of NO by NH_3. *Appl. Catal., B* **2010**, *94*, 71−76.

(12) Chen, L.; Li, J.; Ge, M.; Zhu, R. Enhanced Activity of Tungsten Modified CeO_2/TiO_2 for Selective Catalytic Reduction of NO_x with Ammonia. *Catal. Today* **2010**, *153*, 77−83.

(13) Rusu, C. N.; Yates, J. T. Photochemistry of NO Chemisorbed on TiO_2(110) and TiO_2 Powders. *J. Phys. Chem. B* **2000**, *104*, 1729−1737.

(14) Mikhaylov, R. V.; Lisachenko, A. A.; Shelimov, B. N.; Kazansky, V. B.; Martra, G.; Alberto, G.; Coluccia, S. FTIR and TPD Analysis of Surface Species on a TiO_2 Photocatalyst Exposed to NO, CO, and NO−CO Mixtures: Effect of UV−vis Light Irradiation. *J. Phys. Chem. C* **2009**, *113*, 20381−20387.

(15) Chang, C. J.; Lin, C. K.; Chen, C. C.; Chen, C. Y.; Kuo, E. H. Gas Sensors with Porous Three-Dimensional Framework using TiO_2/Polymer Double-Shell Hollow Microsphere. *Thin Solid Films* **2011**, *520*, 1546−1553.

(16) Lu, G.; Linsebigler, A.; Yates, J. T. Ti^{3+} Defect Sites on TiO_2(110): Production and Chemical Detection of Active Sites. *J. Phys. Chem.* **1994**, *98*, 11733−11738.

(17) Sorescu, D. C.; Rusu, C. N.; Yates, J. T. Adsorption of NO on the TiO_2(110) Surface: An Experimental and Theoretical Study. *J. Phys. Chem. B* **2000**, *104*, 4408−4417.
(18) Abad, J.; Bohme, O.; Roman, E. Dissociative Adsorption of NO on TiO_2(110) Argon Ion Bombarded Surfaces. *Surf. Sci.* **2004**, *549*, 134−142.
(19) Sorescu, D. C.; Yates, J. T. First Principles Calculations of the Adsorption Properties of CO and NO on the Defective TiO_2(110) Surface. *J. Phys. Chem. B* **2002**, *106*, 6184−6199.
(20) Li, J.; Wu, L.; Zhang, Y. Theoretical Study of Adsorbed-Decomposition of NO, CO, and CH_2O on a TiO_2(110) (1 × 1) Defect. *Chem. Phys. Lett.* **2001**, *342*, 249−258.
(21) Abad, J.; Bohme, O.; Roman, E. Dissociative Adsorption of NO on TiO_2(110)-1 × 2 Surface: Ti_2O_3 Rows as Active Sites for the Adsorption. *Langmuir* **2007**, *23*, 7583−7586.
(22) Dohnálek, Z.; Kim, J.; Bondarchuk, O.; Mike White, J.; Kay, B. D. Physisorption of N_2, O_2, and CO on Fully Oxidized TiO_2(110). *J. Phys. Chem. B* **2006**, *110*, 6229−6235.
(23) Henderson, M. A. Structural Sensitivity in the Dissociation of Water on TiO_2 Single-Crystal Surfaces. *Langmuir* **1996**, *12*, 5093−5098.
(24) Kim, Y. K.; Kay, B. D.; White, J. M.; Dohnalek, Z. Alcohol Chemistry on Rutile TiO_2(110): The Influence of Alkyl Substituents on Reactivity and Selectivity. *J. Phys. Chem. C* **2007**, *111*, 18236−18242.
(25) Henderson, M. A. Evidence for Bicarbonate Formation on Vacuum Annealed TiO_2(11O) Resulting from a Precursor-Mediated Interaction between CO_2 and H_2O. *Surf. Sci.* **1998**, *400*, 203−219.
(26) Kim, B.; Li, Z.; Kay, B. D.; Dohnalek, Z.; Kim, Y. K. Unexpected Nondissociative Binding of N_2O on Oxygen Vacancies on a Rutile TiO_2(110)-1 × 1. *J. Phys. Chem. C* **2012**, *116*, 1145−1150.
(27) Wendt, S.; Schaub, R.; Matthiesen, J.; Vestergaard, E. K.; Wahlström, E.; Rasmussen, M. D.; Thostrup, P.; Molina, L. M.; Lægsgaard, E.; Stensgaard, I.; Hammer, B.; Besenbacher, F. Oxygen Vacancies on TiO_2(110) and Their Interaction with H_2O and O_2: A Combined High-Resolution STM and DFT Study. *Surf. Sci.* **2005**, *598*, 226−245.
(28) Oviedo, J.; Sanz, J. F. N_2O Decomposition on TiO_2(110) from Dynamic First-Principles Calculations. *J. Phys. Chem. B* **2005**, *109*, 16223−16226.
(29) Dohnálek, Z.; Lyubinetsky, I.; Rousseau, R. Thermally-Driven Processes on Rutile TiO_2(110)-(1 × 1): A Direct View at the Atomic Scale. *Prog. Surf. Sci.* **2010**, *85*, 161−205.
(30) Henderson, M. A.; Epling, W. S.; Perkins, C. L.; Peden, C. H. F.; Diebold, U. Interaction of Molecular Oxygen with the Vacuum-Annealed TiO_2(110) Surface: Molecular and Dissociative Channels. *J. Phys. Chem. B* **1999**, *103*, 5328−5337.
(31) Ménétrey, M.; Markovits, A.; Minot, C. Adsorption of Chlorine and Oxygen Atoms on Clean and Defective Rutile-TiO_2(110) and MgO (100) Surfaces. *J. Mol. Struct.-Theochem.* **2007**, *808*, 71−79.
(32) Kim, Y. K.; Hwang, C.-C. Photoemission Study on the Adsorption of Ethanol on Clean and Oxidized Rutile TiO_2(110)-1 × 1 Surfaces. *Surf. Sci.* **2011**, *605*, 2082−2086.
(33) Wendt, S.; Sprunger, P. T.; Lira, E.; Madsen, G. K. H.; Li, Z. S.; Hansen, J. O.; Matthiesen, J.; Blekinge-Rasmussen, A.; Laegsgaard, E.; Hammer, B.; Besenbacher, F. The Role of Interstitial Sites in the Ti 3*d* Defect State in the Band Gap of Titania. *Science* **2008**, *320*, 1755−1759.
(34) Yim, C. M.; Pang, C. L.; Thornton, G. Oxygen Vacancy Origin of the Surface Band-Gap State of TiO_2(110). *Phys. Rev. Lett.* **2010**, *104*, 036806.